General Disclaimer

One or more of the Following Statements may affect this Document

- This document has been reproduced from the best copy furnished by the organizational source. It is being released in the interest of making available as much information as possible.

- This document may contain data, which exceeds the sheet parameters. It was furnished in this condition by the organizational source and is the best copy available.

- This document may contain tone-on-tone or color graphs, charts and/or pictures, which have been reproduced in black and white.

- This document is paginated as submitted by the original source.

- Portions of this document are not fully legible due to the historical nature of some of the material. However, it is the best reproduction available from the original submission.

Methods of Reducing Energy Consumption of the Oxidant Supply System for MHD/Steam Power Plants

A. J. Juhasz
National Aeronautics and Space Administration
Lewis Research Center

Methods of Reducing Energy Consumption of the Oxidant Supply System for MHD/Steam Power Plants

A. J. Juhasz
National Aeronautics and Space Administration
Lewis Research Center
Cleveland, Ohio 44135

METHODS OF REDUCING ENERGY CONSUMPTION OF THE OXIDANT SUPPLY SYSTEM FOR MHD/STEAM POWER PLANTS

A. J. Juhasz
NASA-Lewis Research Center
Cleveland, Ohio

Abstract

An in-depth study was conducted to identify possible improvements to the oxidant supply system for combined cycle MHD power plants which would lead to higher thermal efficiency and reduction in the cost of electricity, COE. Results showed that the oxidant system energy consumption could be minimized when the process was designed to deliver a product O_2 concentration of 70 mole percent. The study also led to the development of a new air separation process, referred to as "liquid pumping and internal compression." MHD system performance calculations show that the new process would permit an increase in plant thermal efficiency of 0.6 percent while allowing more favorable tradeoffs between magnetic energy and oxidant system capacity requirements.

I. Introduction

Oxygen enrichment of the MHD combustor oxidant stream at low and intermediate preheat temperatures has been identified as a viable alternative to systems using indirectly fired high temperature air heaters.[1,2,3] These studies identified the attractiveness of MHD/steam power plants using intermediate temperature recuperative preheat and oxygen enrichment of the combustor oxidizer for early commercial MHD power plants. Detailed MHD plant performance calculations considering oxygen enriched MHD combustion air[4] showed that the energy consumption required for oxygen production has a significant impact on the overall results. Although energy consumption values required for oxygen production by air separation plants delivering a high purity oxygen product (above 99 mol percent O_2) range from 280 to 300 kWh/ton of pure O_2, considerable energy savings can be achieved by using a medium purity product (60 to 80 mol percent O_2) for blending with air to produce the required MHD combustor oxidant stream whose oxygen concentration may range from 25 to 40 mol percent.

Such a "medium purity" air separation plant was placed in service by Linde A.G. for the Thyssen Steel Works, Germany, in 1972.[5,6] This plant delivers a 70,000 normal cubic meters per hour (ncmh) (43,500 scfm) product stream at near atmospheric pressure containing 60 mol percent oxygen which is blended with air to form a blast furnace stream of 283 000 ncmh (176,000 scfm) containing 30.6 mol percent oxygen. The plant's specific energy consumption (SEC) is reported at 224 kWh per ton of equivalent pure oxygen (TEPO).

The present study was managed by NASA LeRC for DOE under Interagency Agreement No. DE-AI01-77ET10769. The Lotepro Co. of New York, NY a subsidiary of Linde A.G., FRG (Germany) was the main contractor under contract DEN3-165. Also supplying data were Linde A.G. and a number of industrial compressor manufacturers notably, Demag-Mannesman Co., Dresser Industries, Inc., MAN/GHH Co., Sulzer Brothers, Inc., and Transamerica De-Laval, Inc.

The study objectives and preliminary results have been reported on previously in its early stage.[7] The main objective was to explore process variations for their potential reduction in SEC below the 224 kWh/TEPO quoted above. The work has recently been completed, and a comprehensive report is in preparation. The present paper summarizes the main results of the study, including a brief description of a new air separation process applicable to thermodynamic cycles requiring pressurized oxidant streams, and its effect on the performance of a 500 MW_e combined cycle MHD power plant.

II. Cryogenic Air Separation Process

Before discussing the study results, a brief review of the basic cryogenic air separation process is in order.

Cryogenic air separation processes utilize the difference in boiling points of the various air components (principally N_2 and O_2) and the changes in boiling points with pressure to achieve component separation by fractional distillation. The basic process utilizes a number of auxiliary components (compressors, expanders, heat exchangers, adsorbers, switching valves) whose function is to change the state of the input air stream so that component separation can take place, and also to condition the output streams (product oxygen and nitrogen) to user requirements. The actual separation or rectification process is usually carried out in "double rectification columns" consisting of an upper compartment operated at low pressure (near atmospheric in most cases) and a lower compartment operated at higher pressure. The lower compartment is usually referred to as the medium pressure column, the upper, as the low pressure column. Both columns are equipped with a number of perforated separation trays, the use of which brings about a series of fractional evaporations and condensations between a rising vapor, that is successively enriched in nitrogen, and a falling liquid, which is being enriched in oxygen at each stage. The process requirement for this heat and mass transfer to occur in the two phase-two component countercurrent flow environment dictates the pressure difference between the two columns and thereby specifies the process energy input required for the Air Separation Unit (ASU) air compressor. This is because nitrogen, which at atmospheric pressure has a lower boiling point than the desired product oxygen, must condense at the top of the medium pressure column in order to evaporate product oxygen at the bottom of the low pressure column. The only way this requirement can be met is for the condensation of N_2 to take place at a higher pressure than that of the evaporating product O_2. It should be noted that the higher the desired O_2 concentration (purity) of the product, which is collecting at the bottom of the low pressure column, the greater the pressure difference requirement between the two columns and the higher the compressor power input for the same input air flow.

Basic Air Separation Plant

A schematic of a conventional air separation plant based on the process described above is shown in figure 1. Its main components are:

- Air compressor, (CP)
- Adsorbers for the removal of water and carbon dioxide, (WS, MS1, MS2)
- Expansion turbine for the production of refrigeration, (T)
- Heat exchangers for cooling the air to liquefaction temperature and warming the oxygen and nitrogen products to ambient temperature, (E)
- Rectification columns, (C1 and C2) and condenser-evaporator, (K) for the separation of air into O_2 and N_2 on the basis of vapor-to-liquid heat exchange and mass transfer

In many plants the removal of water and carbon dioxide is combined with the cooling of the air. This is done in reversing heat exchangers or regenerators. The flow paths of the air and product streams can be traced on figure 1. Filtered atmospheric air is compressed in an intercooled and aftercooled air compressor, CP, to a pressure which is determined by the requirements of the particular process, usually 4 to 6 bars. It is then passed through the water separator, WS, and adsorbers, MS, to the heat exchangers, E, and cooled to about 100°K with the aid of expansion turbine, T. The cold air is injected as a saturated vapor into the medium-pressure column, C1, where it is separated into a nitrogen fraction and the so-called rich liquid fraction, which contains about 40 percent oxygen. The separation is obtained by contacting the rising vapor with liquid nitrogen flowing down from the condensor-evaporator, K. This causes the liquid collecting in the kettle at the bottom of C1 to become enriched in oxygen while the vapor, which is condensed at the top of C1, is enriched in nitrogen. Both fractions leave C1 in the liquid state and flow through expansion valves to the low-pressure column, C2, where additional rectification to the final product purity takes place. Both nitrogen and product oxygen leave column C2 in the gaseous state at near atmospheric pressure and are heated in heat exchanger E before being ducted to the user. Note that for applications, such as MHD, requiring lower O_2 concentrations than those of typical medium purity ASU products, the product stream is mixed with atmospheric air before compression in specially designed uncooled oxygen-enriched air compressors as indicated by oxidant compressor, OC, in figure 1. Moreover, as shown in the appendix at the end of this paper, the mixing of air separation plant product and air, to obtain mixtures containing certain mole percentages of O_2, will result in slightly different mixture compositions than those obtained by mixing pure oxygen with air.

III. Process Study and Results

Summary of Process Variations

The approach used was to do a systematic analysis of as many as 18 process variations for an oxidant supply system sized for a 1000 MW_e MHD/steam power plant. The oxidant supply system included the air separation plant as well as the final oxidant mixing chamber and oxygen enriched air compressor. Delivery pressure of the oxidant stream to the MHD combustor was specified at 8 atm and the O_2 concentration of the oxidant stream was 30.6 mol percent. The process parameters varied in the study were product O_2 concentration which was ranged from 30.6 to 99.5 mol percent O_2, and the upper column pressure which was varied from 1 atm to 8 atm, with the high pressure cases also providing pressurized N_2 for power recovery. For each process studied both total power consumption and relative cost figures were obtained.

Results showed that the atmospheric upper column pressure cases, in which the product is mixed with ambient air prior to compression to combustor pressure, were superior to the high pressure upper column cases, both in total power consumption and in capital cost.[7] Figure 2 shows specific energy consumption, SEC, as a function of product purity for the atmospheric product cases. Note that the results represent a tradeoff between the ASU input air compressor pressure ratio requirement, which increases with product purity, and the ASU input air compressor flow requirement, which decreases with product purity. The SEC is shown to drop from 255 kWh/TEPO at 40 percent product purity to 195 kWh/TEPO at 70 to 80 percent purity and increase to near 240 kWh/TEPO for the high purity product. Hence the optimum (minimum compressor power) tradeoff between compressor flow and pressure ratio occurs at product purities between 70 to 80 percent. Since MHD applications require combustor oxidant O_2 concentrations (25 to 40 mole percent) well below the product purities at which compressor power is minimized, the more efficient medium purity air separation processes are compatible with MHD/steam power cycles. Based on these results a plant delivering a 70 mol percent O_2 product at one atmosphere was chosen for use in the 200 MW_e Engineering Test Facility (ETF) Conceptual Design.[8]

New Air Separation Process

Having considered the available variations of the basic process exemplified by the Thyssen Steel plant,[5] we decided to explore the potential additional improvement in total power consumption for a process which utilizes pumping of the product in the liquid state to the final end use pressure, product vaporization at this pressure, followed by heating and mixing with a separately compressed air stream to obtain the desired oxidant O_2 concentration. Such a process may have significant advantages for end uses that require the process output stream to be delivered at a pressure which is above atmospheric. The conceptual design for such a process was developed jointly by NASA LeRC and Lotepro. The process is referred to as an "Internal Compression and Liquid Product Pumping" in an invention disclosure currently being prepared.

Process Energy Consumption

To evaluate the potential advantages of the new process over the previously discussed optimized conventional process a study was conducted of two oxidant supply systems, sized for a 500 MW_e MHD/steam plant, using the new process and the optimized conventional process. A comparison of

power consumption results and of the main process parameters is shown in tables I and II. Also, a block diagram comparing the main features of the two oxidant supply systems is shown in figure 3.

Results in table I show that the new process, in which the product from the upper column is pumped as a liquid to the desired pressure, evaporated and heated, and then mixed with air compressed in the blend air compressor, has a lower overall energy consumption than the optimized conventional process in which an atmospheric pressure product is mixed with ambient air and the resulting oxidant stream is compressed in the oxidant compressor (see figure 3). Note that the oxidant compressor (an axial/radial machine) must be rated for oxygen enriched air service which implies a small penalty on efficiency and cost, whereas the blend air compressor used in the new process only has to compress air, which is less hazardous, and therefore can be compressed more efficiently in a multi-stage axial machine.

Table II shows that for the particular oxidant pressure of 7.22 atm the actual SEC of 267 kWh/TEPO (specified at full oxidant pressure) for the new process is higher than the SEC of 195 kWh/TEPO (specified at atmospheric pressure) for the optimized conventional process. However, the overall energy consumption is lower for the new process, because the product is already at oxidant pressure and only the blend air stream has to be compressed to this pressure. Also, as mentioned above, a more efficient compressor can be used for the blend air stream than for the oxygen enriched air stream of the conventional process. The total energy consumption of the new process can also be obtained by treating it as an optimized conventional process which has an SEC of only 177.5 kWh/TEPO. This equivalent SEC obtained for an oxidant pressure of 7.22 atm is plotted as a triangle in figure 2.

To compute the energy consumption for the new process at other oxidant pressures the reader is referred to figure 4. Here both the actual SEC and the equivalent SEC are plotted for oxidant pressures ranging from ambient to 8.0 atmospheres. The plotted data points represent results of detailed calculations. The plots show that while an oxidant pressure increase from 2 to 8 atmospheres produces a nearly linear rise in actual SEC, the equivalent atmospheric SEC is practically constant at about 175 kWh/TEPO. Note that the equivalent SEC values have been adjusted upward to include a penalty for the final oxidant temperature being up to 40K (70F) lower than for the optimum conventional process. However, this penalty could be decreased gradually for oxidant supply pressures above 8.5 atmospheres. This is because safety considerations require that the oxygen enriched air compressors of the conventional process be cooled to keep discharge temperatures below 590K (600F). As a result the equivalent SEC values would decrease to 160 kWh/TEPO at oxidant pressures of 10 atmospheres and above.

Air Separation Plant Sizing and Capital Cost

Care must be taken to determine the lowest acceptable O_2 content in the oxidant in order to minimize the oxidant plant cost. For the 500 MW$_e$ MHD plant, the ASU was conservatively sized for 4250 tons/day of contained oxygen in order to deliver a 35 mol percent O_2 stream to the combustor. Figure 5 is a semi-logarithmic plot, which shows how the required O_2 tonnage increases with O_2 mol fraction in the oxidant, $\mathfrak{X}$. The figure also shows that the required ASU capacity is directly proportional to the "percent oxygen enrichment" parameter, PCTE (congruent curve displaced by a constant). The PCTE parameter is defined and its use is explained in the appendix.

To permit translation of the plant capacity figures to capital cost requirements, figure 6 shows the specific cost figures in 1978 dollars/ton per day of plant size. These figures assume overnight construction cost (ONCC) for the basic air separation plant without oxidant compressors. The 1978 dollar values are used for reasons of compatibility with previously completed MHD studies.[1,2] However, the cost figures can be translated to more recent time periods by using utility construction cost escalation rates.[9]

The specific cost curve of figure 6 shows that in the construction of large air separation plants there is a cost advantage in using a large single train configuration (up to 6500 tons/day of contained O_2), rather than following the customary multiple parallel train approach. The tradeoff is between column rail shippability, overall system redundancy and the need for on-site fabrication of the large columns required. Relative costs for two air separation units using the new process to deliver the 4250 tons/day of contained O_2, required for the 500 MW$_e$ plant, are shown in table III. One unit is based on the use of three trains and rail shippable columns of 13.5 ft diameter. The other is based on a field constructed single train with a 24.3 ft column diameter. The table shows that even though the single train requires on-site fabrication, the reduction in total number of components results in a relative capital cost savings of 11 percent.

IV. Calculation of 500 MW$_e$ MHD Power Plant Performance

The MHD plant performance was calculated following the methods described in previous papers.[4,10] The power plant major cycle parameters are listed in table IV and the generator constraints are shown in table V. The bottom cycle performance was calculated using the PRESTO computer code.[11] The bottom cycle is based on the one discussed in the AVCO CSPEC,[12] with steam conditions of 2400 psig/1000F/1000F. The channel was cooled using low pressure, low temperature feedwater. The oxidant compressor and ASU compressors are assumed to be driven by a single steam turbine.

The generator operating conditions were selected to optimize the performance of the overall combined cycle power plant. This procedure was carried out for oxygen concentrations of 25, 30 and 35 mol percent in the oxidant, MPO, (i.e. $\mathfrak{X} \cdot 100$), and channel lengths of 10 m, 15 m and 20 m.

The overall plant thermal efficiency is plotted as a function MPO for the channel lengths considered in figure 7. Results are shown (figure 5a), for an air separation plant SEC of 224 kWh/TEPO, representing the Thyssen steel plant ASU technology and also for the new process (equivalent SEC of

3

177.5 kWh/TEPO) (figure 7b). The power plant thermal efficiencies are shown to be up to 0.7 percent higher for plants using the new process (figure 7b). Also, the oxidant O_2 concentration at which the maximum efficiency occurs (dashed curve) shifts to slightly higher levels. Thus, for the conventional process and a 15 m channel the maximum efficiency is about 43.7 percent, and it occurs at an MPO of 32 mol percent, (figure 7a), whereas for the new process it rises to 44.3 percent at an MPO of 33.5 mol percent, (figure 7b). Note that use of the optimized conventional air separation process (195 kWh/TEPO), incorporated in the ETF and the CSPEC studies, would result in overall thermal efficiency values that are about halfway between the values given above.

For both the higher and lower energy consumption, figure 7 shows that there are tradeoffs between plant thermal efficiency, oxidant O_2 concentration and channel length. An additional tradeoff is shown in figure 8, which is a plot of magnetic energy stored in the channel volume as a function of plant thermal efficiency for the various oxidant O_2 mole fractions and channel lengths considered. The magnetic energy is proportional to magnet costs while the MPO can be related to costs associated with the oxidant supply system, as indicated in figure 5. Therefore these parameters should be minimized in an optimally designed combined cycle MHD plant, consistent with sufficiently high thermal efficiency, in order to achieve the lowest cost of electricity, COE. Comparison of figures 8a and 8b shows that not only is the thermal efficiency higher at all conditions for the lower oxygen production energy, but also that a given decrease in magnetic energy will result in a smaller sacrifice in thermal efficiency for the plant with the lower oxygen production energy requirement. For example, the plant thermal efficiency is about 44.40 percent (figure 8b) using a 20 m channel and an oxidant O_2 mol fraction of 0.30. For these conditions the magnetic energy is about 1150 megajoules (MJ). Reducing the channel length to 15 m, but increasing the O_2 mol fraction, x, to near 0.35 (actually 0.335 as per figure 7b) will result in a thermal efficiency of 44.27 percent, a loss of only 0.13 percent from the 44.4 percent figure quoted above. But the magnetic energy decreases dramatically from 1150 MJ to 675 MJ, equivalent to a 41 percent decrease. Of course, the above tradeoff implies an increase in the oxidant supply system capacity of about 24 percent.

The same tradeoff, based on the results shown in figure 8a for the higher oxygen production energy requirement, will result in a power plant thermal efficiency drop from 43.90 to 43.60 percent, the resulting loss of 0.3 percent being more than double the value quoted above.

Final system optimization will require additional studies of the type discussed above, once the relationship between component sizes and associated dollar values can be defined more clearly. However, the results of this study point out that one can obtain higher overall thermal efficiencies by using large, advanced technology, oxidant supply systems which offer significant savings in oxygen production costs. These systems will also allow more flexibility in the overall power plant optimization and therefore contribute in the attainment of the lowest potential COE for combined cycle MHD/steam power plants.

V. Concluding Remarks

The results of this study show that the oxidant production cost for a combined cycle MHD/steam power plant can be lowered by improvements to the oxidant supply system. A new air separation process based on internal compression and liquid pumping and configured for a 500 MW$_e$ MHD/steam power plant with a 7.22 atm oxidant delivery pressure was shown to achieve a 21 percent drop in total energy consumption below state of the art, medium purity air separation plants operating overseas. The new process also was shown to achieve a 10 percent reduction below the energy requirement of optimized conventional technology air separation plants assumed for the CSPEC study (195 to 175 kWh/TEPO).

For the 500 MW$_e$ power plant, the reduced energy consumption for oxidant production was shown to result in an overall thermal efficiency increase of 0.6 percent which, when combined with projected capital cost savings identified in the study could bring about reasonable reductions in the plant COE.

References

1. Hals, F. A.: Parametric Study of Potential Early Commercial MHD Power Plants. NASA CR-159633, DOE/NASA/0051-79/1, 1979.

2. Marston, C. H.; et al.: Parametric Study of Potential Early Commercial MHD Power Plants, NASA CR-159634, DOE/NASA/0052-79/1, 1980.

3. Staiger, P. J.; and Abbott, J. M.: Summary and Evaluation of the Parametric Study of Potential Early Commercial MHD Power Plants (PSPEC). NASA TM-81497, DOE/NASA/2674-8019, 1980.

4. Pian, C. C. P.; Staiger, P. J. and Seikel, G. R.: MHD Performance Calculations with Oxygen Enrichment. NASA TM-79140, DOE/NASA/2674-79/4, 1979.

5. Schoenpflug, E.: The Blast-Furnace Oxygen Plant at Schwelgern. Linde Reports on Science and Technology, vol. 18, 1973, pp. 27-28.

6. Rueckborn, G.: Oxygen Enrichment: Cost and Effectiveness. Cryogenics and Industrial Gases, vol. 6, no. 4, July/Aug. 1971, pp. 27-30.

7. Springmann, H.; Greenberg, R.; and Juhasz, A. J.: The Optimization of Air Separation Plants for Combined Cycle MHD-Power P ant Applications. NASA TM-81510, DOE/NASA/2674-80/10, 1980.

8. Hartwig, W.; and Greenberg, R.: System Design Description (SDD-501) Oxidant Supply System of Magnetohydrodynamics Engineering Test Facility Conceptual Design - 200 MW$_e$ Power Plant. Conceptual Design Engineering Report (CDER), DOE/NASA/0224-1, NASA CR-165452, vol. V, Sept. 1981.

9. Handy-Whitman Index of Public Utility Construction Costs, Bulletin 115. Whitman, Requard and Associates, 1982.

10. Staiger, P. J.: Performance Calculations for 200-1000 MW$_e$ MHD/Steam Power Plants. NASA TM-81775, DOE/NASA/10769-16, 1981.

11. Fuller, L. C.; and Stovall, T. K.: User's Manual for PRESTO - A Computer Code for the Performance of Regenerative Superheated Steam Turbine Cycles. (ORNL-5547, Oak Ridge National Lab.; C-10669-D W-7405-Eng-26) NASA CR-159540.

12. Hals, F. A.: Conceptual Design Study of Potential Early Commercial MHD Power Plant. NASA CR-165235, DOE/NASA/0051-2, March 1981.

13. Comparative Evaluation of Phase I Results from the Energy Conversion Alternative Study (ECAS). NASA TMX-71855, 1976.

TABLE I: AIR SEPARATION POWER CONSUMPTION COMPARISON FOR 500 MW$_e$ PLANT

	OPTIMIZED CONVENTIONAL PROCESS*	NEW PROCESS
INPUT AIR COMPRESSOR, KW	30,590	29,630
BOOST AIR COMPRESSOR, KW	0	13,410
EXPANSION TURBINE (RECOVERY), KW	-620	-781
PRODUCT PUMP, KW	0	86
BLEND AIR COMPRESSOR, KW	0	36,135
OXIDANT COMPRESSOR, KW	52,990	0
TOTAL POWER CONSUMPTION, KW	82,960	78,480

TABLE II: AIR SEPARATION PROCESS PARAMETER COMPARISON FOR 500 MW$_e$ PLANT

	OPTIMIZED CONVENTIONAL PROCESS	NEW PROCESS
Input Air Flow, nm^3/sec*	154.75	154.75
Input Air Pressure, atm	3.95	3.93
Boost Air Flow, nm^3/sec	---	63.89
Boost Air Pressure, atm	---	15.99
Boost Air Temp, K	---	455
Upper Column Pressure, atm	1.0	1.0
Product O$_2$ Content, mol pct.	70	70
Product Pressure, atm	1.0	7.22
Product Flow, nm^3/sec	44.7	44.7
Product Flow, tons O$_2$/day	4250	4250
Blend Air Flow, nm^3/sec	111.3	111.3
Blend Air Pressure, atm	1.0	7.22
Blend Air Temperature, K	290	540
Oxidant Flow, nm^3/sec	156.0	156.0
Oxidant O$_2$ Content, mol pct.	35	35
Oxidant Pressure, atm	7.22	7.22
Oxidant Temperature, K	544	515
SEC at Prod. Press, kWh/TEPO	195	267
SEC Corrected to P=1atm, T=544K, kWh/TEPO	195	177.5

* To convert nm^3/sec to scfm, multiply by 2239.5.

TABLE III.: COLUMN SIZE AND CAPITAL COST COMPARISONS FOR TRIPLE VS. SINGLE TRAIN ASU FOR 500 MW$_e$ PLANT

	Triple Train	Single Train
Column Dia,* m(ft)	4.10 (13.5)	7.40 (24.3)
Relative Turnkey Cost	1.00	0.89

*Assumed limit for rail shippability is 4270 mm (14 ft)

TABLE IV: MAJOR CYCLE PARAMETERS

```
Coal type . . . . . . . . . . . . . Montana Rosebud
Moisture content of coal delivered
  to combustor, percent . . . . . . . . . . . . 5
Oxidizer preheat temperature, K (F) . . 867 (1100)
Combustor pressure, atm . . . Selected to maximize
                                     plant efficiency
Combustor heat loss, percent HHV of coal . . . 5
Combustor oxidizer-fuel ratio
  relative to stoichiometric . . . . . . . . 0.90
Combustor slag rejection, percent . . . . . . 80
Generator type . . . . . . . . . . . . . . Faraday
Potassium-coal mass ratio . . . . . . . . . 0.0859
MHD Generator inlet Mach number . . . . . . . 0.8
Diffuser pressure recovery coefficient . . . 0.6
Diffuser exit pressure, atm . . . . . . . . . 1.0
MHD generator length, meters . . . . . 10, 15, 20
Cycle compressor polytropic efficiency . . . 0.90
Sulfur removal by seed, percent . . . . . . . 70
Final oxidizer-fuel ratio relative
  to stoichiometric . . . . . . . . . . . . . 1.05
Stack temperature, F . . . . . . . . . . . . 250
Air separation plant compressor power
  requirement, kW-hr/ton of equivalent
  pure oxygen added . . . . . . . . . . . 224, 178
Pressure drop from compressor exit to
  combustor, percent of compressor
  exit pressure . . . . . . . . . . . . . . . 0.1
```

TABLE V: GENERATOR CONSTRAINTS

```
Maximum axial electric field, kV/m . . . . . 2.5
Maximum transverse electric field, kV/m . . . 4.0
Maximum transverse current density, A/cm$^2$ . . 1.0
Maximum Hall parameter . . . . . . . . . . . 4.0
Maximum magnetic field, T . . . . . . . . . . 6.0
```

APPENDIX: OXIDANT MIXTURE COMPOSITIONS

When air is mixed with the product delivered by medium purity air separation plants the resulting compositions, even at the same O_2 mole fractions, will be different from those of pure oxygen and air mixtures. This is illustrated in tables A1 and A2 which show respective compositions in terms of the mole and mass fractions of the three major constituents, N_2, O_2, and Ar. The air humidity used to compute values of table A2(B) was derived from ECAS[13] conditions.

The reason for the increase in concentration of argon along with that of oxygen in product streams, containing up to 95 mol percent O_2, arises from the fact that the medium purity air separation process removes nitrogen, but not argon, from the product. Argon can be separated from oxygen and collected in high purity plants which use an additional argon separation column.

In MHD applications the concentration of argon in the oxidant stream has a beneficial, albeit small effect on power output, because of the slight increase in plasma conductivity. In addition to composition, tables A1 and A2 also have column tabulations for mixture molecular weight, density, the ratio of contained O_2 to equivalent pure O_2 (which excludes any O_2 contributed by air), and a parameter identified as "Percent O_2 Enrichment",

or PCTE. This parameter has been defined for N_2-O_2 mixtures[4] as

$$PCTE = 100 \times (1 - \frac{N/O}{3.26}) \qquad (1)$$

where N/O is the nitrogen/oxygen mass ratio in the oxidant. Equation (1) has been redefined here for multi-component mixtures as:

$$PCTE = 100 \times (1 - \frac{R/O}{3.32}) \qquad (2)$$

where R/O is the ratio of the sum of non-oxygen mass fractions to the mass fraction of O_2. Since PCTE is directly proportional to O_2 plant capacity, it is a useful parameter for scaling O_2 plant size when the O_2 mol fraction in the oxidant is changed, while keeping the product purity constant. Tables A1 and A2 show PCTE values for O_2 mol fractions ranging from 21 to 100 percent for ASU product-air and pure O_2-air mixtures, respectively. If the product purity is changed, the O_2 plant capacity scales inversely as the ratio of the new-to-old PCTE value. Alternately, for a change in product purity, the new air separation plant capacity can be computed by multiplying the old capacity by the direct ratio of "Contained O_2/pure O_2" values in tables A1 or A2.

TABLE A1: AIR SEPARATION PLANT PRODUCT MIXTURE COMPOSITION

MOLE PERCENT			MASS PERCENT			MOLECULAR	DENSITY	CONT.O2/	PERCENT O2
OXYGEN	NITROGEN	ARGON	OXYGEN	NITROGEN	ARGON	WEIGHT	KG/M*3	PURE O2	ENRICHMENT
21.00	78.064	.936	23.202	75.506	1.291	28.962	1.2921	306.1240	.327
25.00	73.885	1.115	27.450	71.022	1.528	29.143	1.3002	4.8990	20.412
30.00	68.663	1.337	32.687	65.494	1.819	29.368	1.3102	2.6325	37.987
31.00	67.618	1.382	33.725	64.398	1.877	29.414	1.3123	2.4497	40.822
32.00	66.573	1.427	34.759	63.306	1.935	29.459	1.3143	2.2999	43.479
33.00	65.529	1.471	35.791	62.217	1.992	29.504	1.3163	2.1751	45.976
34.00	64.484	1.516	36.819	61.132	2.049	29.549	1.3183	2.0693	48.325
35.00	63.440	1.560	37.844	60.050	2.106	29.594	1.3203	1.9786	50.541
40.00	58.217	1.783	42.923	54.689	2.389	29.820	1.3304	1.6679	59.956
45.00	52.994	2.006	47.925	49.408	2.667	30.046	1.3405	1.4864	67.279
50.00	47.771	2.229	52.852	44.206	2.942	30.272	1.3506	1.3673	73.137
55.00	42.548	2.452	57.707	39.081	3.212	30.498	1.3606	1.2832	77.930
60.00	37.325	2.675	62.490	34.032	3.478	30.724	1.3707	1.2206	81.924
65.00	32.102	2.898	67.204	29.056	3.740	30.950	1.3808	1.1723	85.304
70.00	26.879	3.121	71.849	24.152	3.999	31.176	1.3909	1.1338	88.201
75.00	21.656	3.344	76.427	19.319	4.254	31.402	1.4009	1.1024	90.712
80.00	16.433	3.567	80.940	14.555	4.505	31.627	1.4110	1.0763	92.909
85.00	11.211	3.789	85.385	9.859	4.752	31.853	1.4211	1.0543	94.847
90.00	5.988	4.012	89.775	5.229	4.997	32.079	1.4312	1.0355	96.570
95.00	.765	4.235	94.100	.663	5.237	32.305	1.4413	1.0192	98.112
96.00	.000	4.000	95.055	.000	4.945	32.317	1.4418	1.0159	98.424
97.00	.000	3.000	96.282	.000	3.718	32.237	1.4382	1.0118	98.837
98.00	.000	2.000	97.516	.000	2.484	32.158	1.4347	1.0077	99.233
99.00	.000	1.000	98.755	.000	1.245	32.078	1.4311	1.0038	99.620
100.00	.000	.000	100.000	.000	.000	31.999	1.4276	1.0000	100.000

TABLE A2:   COMPOSITION OF PURE OXYGEN AND AIR MIXTURES

(A) OXYGEN AND DRY AIR

MOLE PERCENT			MASS PERCENT			MOLECULAR WEIGHT	DENSITY KG/M*3	CONT.O2/ PURE O2	PERCENT O2 ENRICHMENT
OXYGEN	NITROGEN	ARGON	OXYGEN	NITROGEN	ARGON				
21.00	78.035	.933	23.198	75.466	1.287	28.967	1.2943	327.5028	.305
25.00	74.083	.886	27.472	71.267	1.216	29.120	1.2992	4.8789	20.497
30.00	69.145	.827	32.750	66.080	1.127	29.312	1.3077	2.6203	38.164
31.00	68.157	.815	33.797	65.051	1.110	29.350	1.3094	2.4382	41.014
32.00	67.169	.803	34.842	64.025	1.092	29.389	1.3111	2.2891	43.685
33.00	66.181	.792	35.884	63.001	1.075	29.427	1.3129	2.1648	46.195
34.00	65.193	.780	36.923	61.980	1.057	29.466	1.3146	2.0595	48.557
35.00	64.206	.768	37.960	60.961	1.040	29.504	1.3163	1.9691	50.784
40.00	59.267	.709	43.102	55.908	.954	29.696	1.3248	1.6598	60.248
45.00	54.328	.650	48.179	50.920	.869	29.888	1.3334	1.4791	67.610
50.00	49.389	.591	53.190	45.996	.785	30.080	1.3420	1.3606	73.499
55.00	44.450	.532	58.138	41.134	.702	30.272	1.3505	1.2769	78.317
60.00	39.511	.473	63.024	36.333	.620	30.464	1.3591	1.2146	82.333
65.00	34.572	.414	67.849	31.592	.539	30.656	1.3677	1.1665	85.730
70.00	29.633	.354	72.613	26.911	.459	30.847	1.3762	1.1281	88.642
75.00	24.694	.295	77.319	22.287	.380	31.039	1.3843	1.0969	91.156
80.00	19.756	.236	81.966	17.720	.302	31.231	1.3933	1.0710	93.375
85.00	14.817	.177	86.557	13.209	.225	31.423	1.4019	1.0491	95.323
90.00	9.878	.118	91.093	8.752	.149	31.615	1.4105	1.0303	97.055
95.00	4.939	.059	95.573	4.350	.074	31.807	1.4190	1.0141	98.605
96.00	3.951	.047	96.463	3.476	.059	31.845	1.4207	1.0112	98.896
97.00	2.963	.035	97.350	2.604	.044	31.884	1.4225	1.0083	99.180
98.00	1.976	.024	98.236	1.734	.030	31.922	1.4242	1.0054	99.459
99.00	.988	.012	99.119	.866	.015	31.961	1.4259	1.0027	99.732
100.00	.000	.000	100.000	.000	.000	31.999	1.4276	1.0000	100.000

TABLE A2:   CONCLUDED

(B) OXYGEN AND HUMID AIR (1.02 MOL PCT H2O)

MOLE PERCENT			MASS PERCENT			MOLECULAR WEIGHT	DENSITY KG/M*3	CONT.O2/ PURE O2	PERCENT O2 ENRICHMENT
OXYGEN	NITROGEN	ARGON	OXYGEN	NITROGEN	ARGON				
21.00	77.029	.921	23.282	74.760	1.275	28.863	1.2877	62.5358	1.599
25.00	73.128	.874	27.565	70.587	1.203	29.022	1.2948	4.6450	21.528
30.00	68.253	.816	32.853	65.433	1.116	29.220	1.3036	2.5663	38.967
31.00	67.278	.804	33.902	64.411	1.098	29.260	1.3054	2.3935	41.779
32.00	65.303	.793	34.948	63.392	1.081	29.300	1.3072	2.2514	44.416
33.00	65.328	.781	35.992	62.375	1.063	29.339	1.3089	2.1325	46.893
34.00	64.353	.769	37.032	61.361	1.046	29.379	1.3107	2.0315	49.224
35.00	63.378	.758	38.070	60.350	1.029	29.419	1.3125	1.9447	51.422
40.00	58.503	.699	43.217	55.334	.943	29.617	1.3213	1.6457	60.764
45.00	53.628	.641	48.295	50.385	.859	29.816	1.3302	1.4699	68.030
50.00	48.752	.583	53.306	45.502	.776	30.014	1.3390	1.3542	73.843
55.00	43.877	.525	58.252	40.683	.694	30.213	1.3479	1.2723	78.599
60.00	39.002	.466	63.133	35.926	.613	30.411	1.3568	1.2112	82.562
65.00	34.127	.408	67.950	31.232	.532	30.610	1.3656	1.1653	85.915
70.00	29.251	.350	72.706	26.598	.453	30.808	1.3745	1.1263	88.790
75.00	24.376	.291	77.400	22.023	.375	31.007	1.3833	1.0955	91.281
80.00	19.501	.233	82.035	17.506	.298	31.205	1.3922	1.0700	93.461
85.00	14.626	.175	86.612	13.047	.222	31.404	1.4010	1.0484	95.384
90.00	9.750	.117	91.131	8.643	.147	31.602	1.4099	1.0299	97.094
95.00	4.875	.058	95.593	4.295	.073	31.801	1.4187	1.0140	98.623
96.00	3.900	.047	96.479	3.431	.059	31.840	1.4205	1.0110	98.910
97.00	2.925	.035	97.362	2.570	.044	31.880	1.4223	1.0082	99.191
98.00	1.950	.023	98.244	1.711	.029	31.920	1.4241	1.0054	99.466
99.00	.975	.012	99.123	.855	.015	31.959	1.4258	1.0026	99.736
100.00	.000	.000	100.000	.000	.000	31.999	1.4276	1.0000	100.000
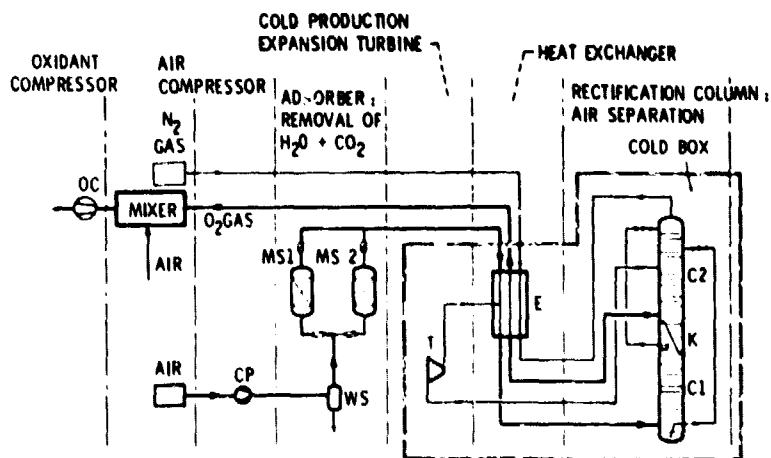
Figure 1. - Basic air separation plant delivering product O_2 at atmospheric pressure.
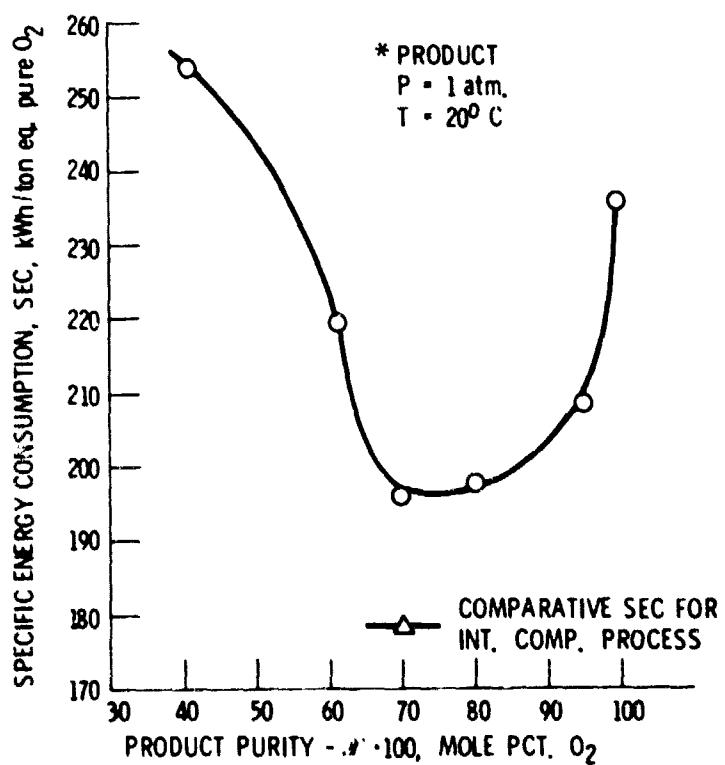
Figure 2. - Air separation process study results (Contract DEN 3-165).

(a)

(b)
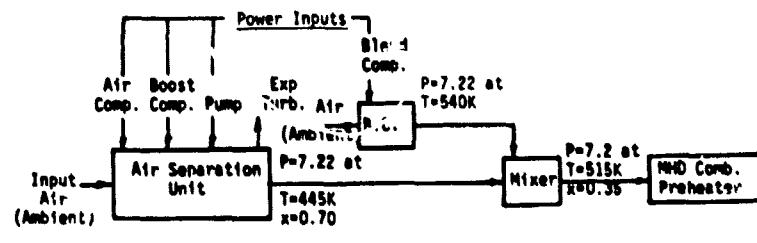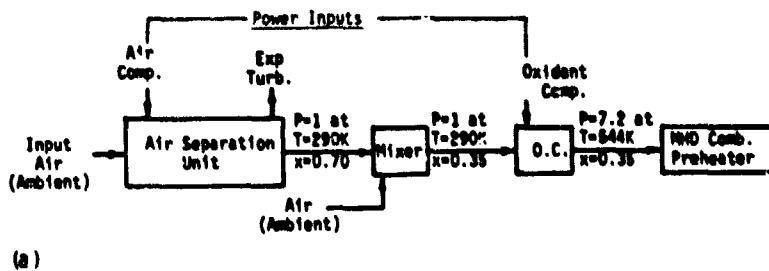
(a) Optimized conventional process.
(b) New process.

Figure 3. - Comparative block diagrams for 500 MW$_e$ MHD oxidant supply systems.
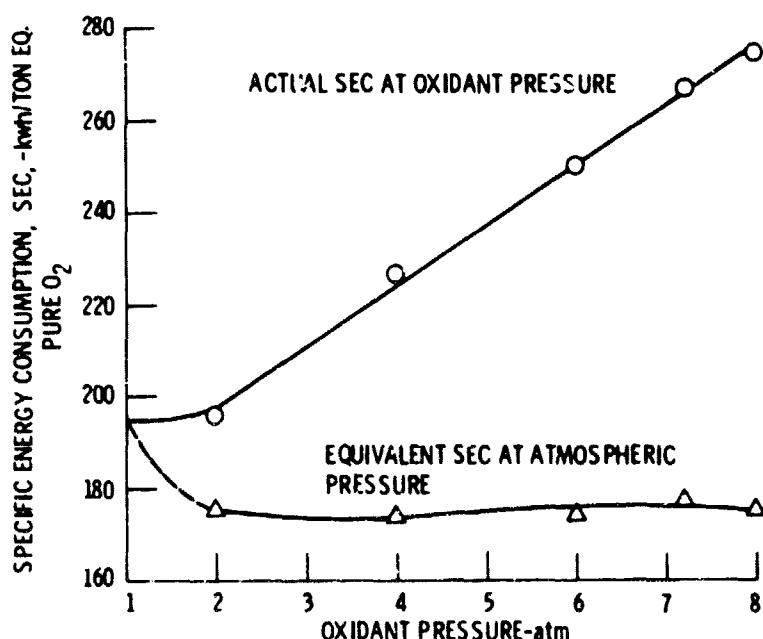
Figure 4. - Specific energy consumption for new air separation process for a range of oxidant pressures.
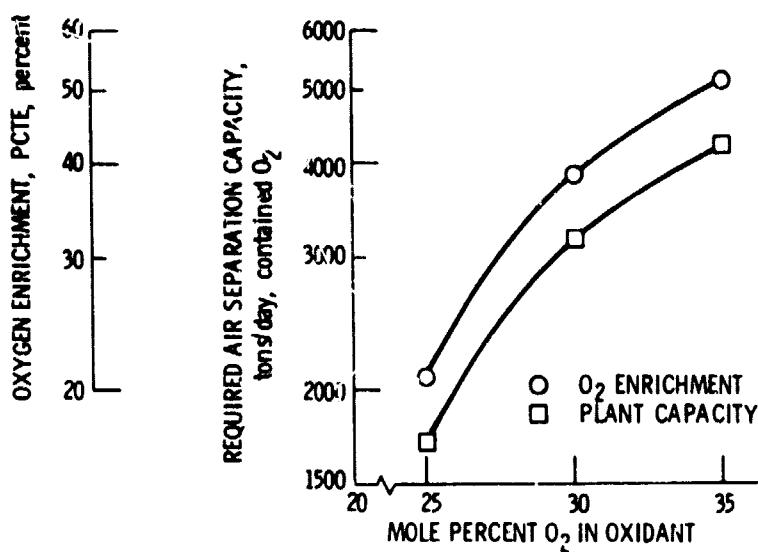
Figure 5. - Air separation plant size variation for 500 MW_e MHD/ steam plant. Product O_2 concentration is 70 mole percent.
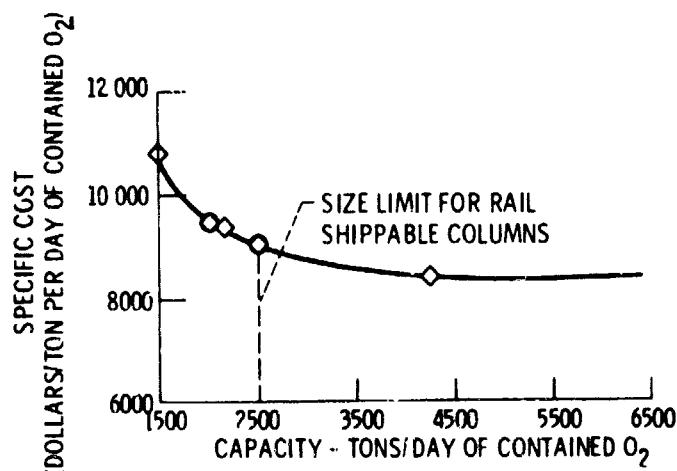

Figure 6. - Air separation plant costs for a range of plant capacities. Product purity of 70 percent assumed. Specific costs are based on mid 1978 ONCC figures.
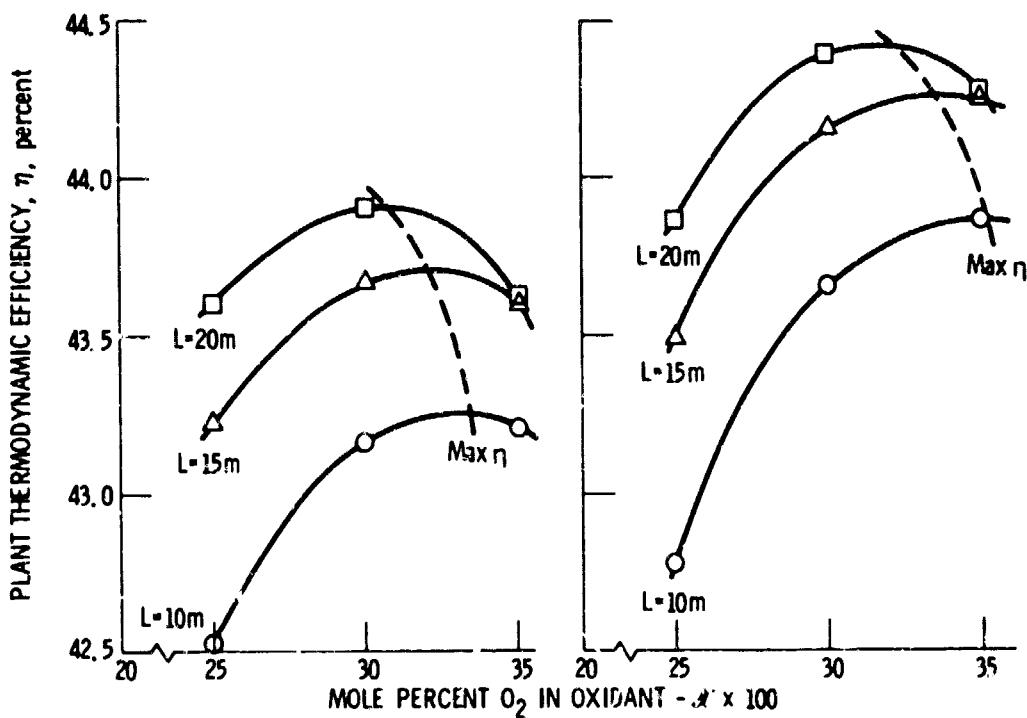
(a) Oxygen production energy is 224 kW-hr/ton of pure O_2.

(b) Oxygen production energy is 178 kW-hr/ton of pure O_2.

Figure 7. - 500 MW_e MHD plant performance for various oxidant mixtures and channel lengths.
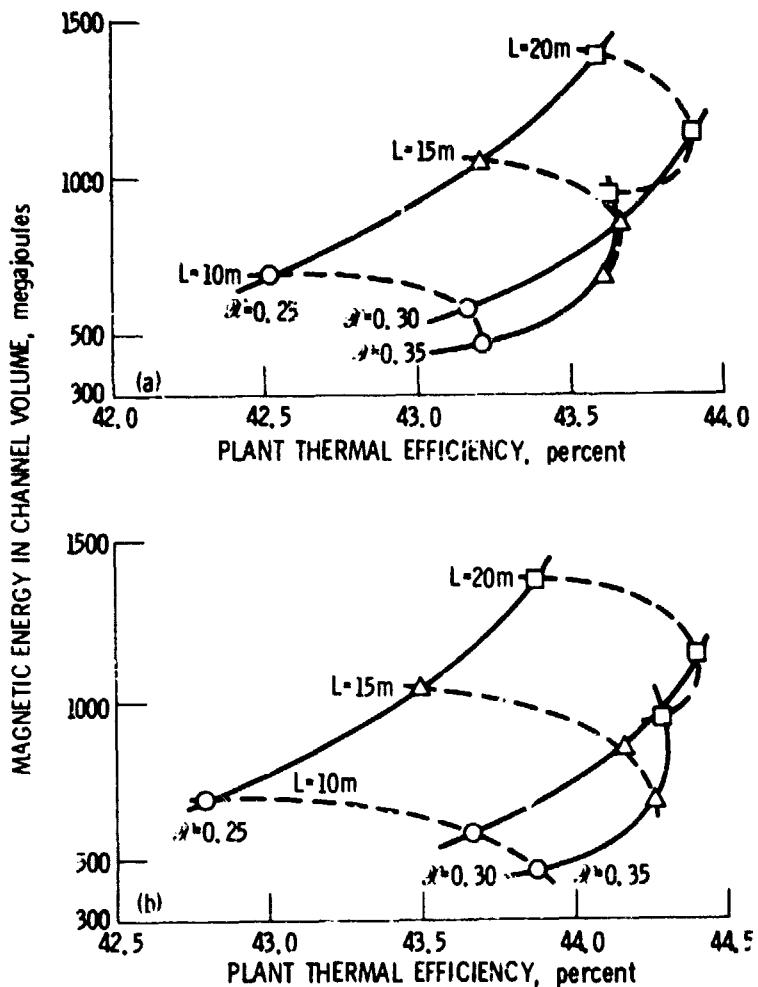
(a) Oxygen production energy is 224 kW-hr/ton of pure O_2.

(b) Oxygen production energy is 178 kW-hr/ton of pure O_2.

Figure 8. - 500 MW$_e$ MHD plant optimization considering: magnet capacity, oxidant system capacity ($\propto \mathcal{N}$), and channel length, L.